HITTITE JOURNAL OF SCIENCE AND ENGINEERING

e-ISSN: 2148-4171
Volume: 11 • Number: 2
June 2024

Sensitivity Analysis of Wear on Metal-On-Metal Bearing Couples via Verification of Numeric and Analytic Methods

Alican Tuncay Alpkaya | Senay Mihcin

Department of Mechanical Engineering, İzmir Institute of Technology, 35433, İzmir, Türkiye.

Corresponding Author

Senay Mihcin
E-mail: senaymihcin@iyte.edu.tr Phone: +00 (232) 750 67 07
RORID: https://ror.org/03stptj97

Article Information

Article Type: Research Article
Doi: https://doi.org/10.17350/10.17350/HJSE19030000332
Received: 19.01.2024
Accepted: 07.05.2024
Published: 30.06.2024

Cite As

Alpkaya AT, Mihcin S. Sensitivity Analysis of Wear on Metal-On-Metal Bearing Couples via Verification of Numeric and Analytic Methods. Hittite J Sci Eng. 2024;11(2):57-67.

Peer Review: Evaluated by independent reviewers working in at least two different institutions appointed by the field editor.
Ethical Statement: Not available.
Plagiarism Checks: Yes - iThenticate
Conflict of Interest: Authors approve that to the best of their knowledge, there is not any conflict of interest or common interest with an institution/organization or a person that may affect this study.

CRediT Author Statement:
Alican Tuncay Alpkaya: Author: Conceptualization, Methodology, Software, Validation, Writing- original draft. **Senay Mihcin:** Author: Data curation, Visualization, Investigation, Validation, Supervision, Writing-review and editing.

Sensitivity Analysis of Wear On Metal-On-Metal Bearing Couples Via Verification of Numeric and Analytic Methods

Alican Tuncay Alpkaya | Senay Mihcin*

Department of Mechanical Engineering, İzmir Institute of Technology, 35433, İzmir, Türkiye.

Abstract

Wear mechanism is important since it leads to revisions in Total Hip Replacement (THR) surgeries. Contact pressure plays an important role in wear mechanisms and needs to be investigated in detail to obtain more accurate wear predictions to understand the wear performance of the implant in the design stage. This study proposes a methodology for verification of contact pressure and pressure distribution via numeric and analytic methods to be used in wear calculations. Based on Hertz's contact theory, the contact pressure and the contact area are calculated in the analytical method. The results are compared to the numeric method's results obtained from the finite element method. The linear and volumetric wear rates of bearing couples' surfaces were estimated by Archard's wear equation. The effect of design parameters on pressure such as head radius, cup thickness, material combination of bearing couples, coating film material, and film thickness are investigated in this study using the proposed methodology. The minimum error between the analytical and numerical results was 0.24% for 28 mm of head diameter, while the maximum error was 11.79 % for 48- mm of head diameter. The minimum contact pressure values were obtained from 48- mm of head radius at a half contact angle of 190 (degrees) in FEM and Hertz calculations, respectively. The maximum linear wear rate was calculated at 0.0026 mm/Mc at a 1- mm cup thickness, while minimum linear wear rate was 0.0022 mm/Mc at a 10- mm cup thickness in the numeric method. The maximum survival cycles of coating materials rate were 31847 cycles for the Stainless-steel coated cup with 500 µm of coating thickness, while the minimum cycles was 2359 cycles for the Ti64 coated cup surface with 100 µm of coating thickness. It is concluded that the most important design parameters are the cup thickness and the material combinations since they have a significant effect on the contact pressure and the contact area. This study provides a verification methodology for the parametric sensitivity analysis before experimental validations. The methodology utilized in this study could be utilized by designers while optimizing the design parameters to minimize the wear.

Keywords: Hertz contact theory, Archard's wear law, linear and volumetric wear rates, finite element analysis, parametric design of hip implants

INTRODUCTION

Total Joint Replacement (TJR) applications started with Sir John Charney in 1958, using metal-on-polymer implants for hip joints (1). Polytetrafluoroethylene (PTFE) was chosen as the acetabular cup material and stainless steel was used as the femoral head material. However, this bearing combination produced excessive wear of PTFE, resulting in a lifespan of two-years (2). This problem led to the research for more durable bearing combinations so that the first metal-on-metal (MoM) bearing couple was introduced by Haboush (US), McKee, and Watson-Farrar (UK) in 1951 (3). Since then, metal-on-metal (MoM) bearing couple has been in use frequently in hip implant applications, due to their outstanding mechanical properties such as higher corrosion resistance, toughness, strength, ease of machinability, cost-effectiveness, and lower surface roughness (4,5). Although the volumetric wear rate of metals in million cycles is higher than that of ceramic materials, the wear rates of ceramics in long term might induce osteolysis (6).

According to the results of National Joint Registry (NJR) (7), 1,091,892 total hip replacements have been performed in the UK, out of which resulted in 31,410 (2.9%) first revision surgeries. These first revision surgeries were due to aseptic loosening, (7,644) adverse soft tissue reaction to debris (5,114), dislocation/subluxation (5,383), pain (4,705), and infection (4,555). To avoid high levels of debris, reduction of coefficient of friction was aimed for longer-lasting joints. To overcome these encountered revision problems, the coating of the bearing surfaces was considered. Thin film coatings on bearing surfaces were investigated for the effects of contact pressure, wear rate, and damage (7). Reinforced hydroxyapatite (HA) coating was used over titanium alloy for orthopedic applications using the plasma spraying technique (7). The HA-based coating film thickness was approximately 100-125 um demonstrating enhanced mechanical properties of wear and corrosion resistance, and bioactivity (7). However, so far there has been no consensus over the optimum film thickness parameters.

Ceramic on ceramic bearing couple contact mechanics of hip implants has been investigated for the effects of changing the head diameter, radial clearance, and loading magnitude (8,9). In another study, the effects of changing the stem geometries and the neck length on wear estimation of the bearing surfaces were investigated in MoM(10,11). Similarly, the contact mechanics of hard-on-hard bearing couples in THR have been investigated in the literature However, in these studies, only a small range of parameters was covered for the investigation of head diameter, clearance, and material combination of ceramics on ceramics, and coating materials were chosen as ceramics (8–13). Previously, the researchers have studied the optimization of design parameters and the material selection for hip implants (14–16). Although there are many studies on investigating the effect of changing the clearance, loading values, and head radius of THR in literature (8–13,17), the parameters of cup thickness for MoM hip implants, coating material, and its thickness, and also material combinations of head-on-cup bearing couple thickness have not been investigated so far in this level. Since computational methods could be costly, it is very important to provide a verification method before moving on to the simulator simulations where experimental validations are compared against the computational results.

Hertz's contact theory (18) is chosen as the analytical model to be utilized for the contact pressure calculations in the prototypes. This theory is mostly used in calculating the contact pressure values, especially on spherical contact surface models. In this study, contact pressure, pressure distribution, and contact area of all bearing prototypes are calculated by using both analytical and numerical methods. An analytical method makes use of the mathematical equations to predict the contact pressure and its distribution, while the numerical

method makes use of the Finite Element Modelling (FEM) technique. The comparison of these two methods and their errors are calculated by changing the design parameters of MoM-bearing couples. These results were used for predicting the linear and volumetric wear rates of bearing surfaces. Estimating the linear and volumetric wear rates could lead the way to calculate the lifespan of hip implants. Since the wear rate has direct effect on overall longevity of hip prosthesis, to quantify this effect, Archard wear equation is utilized to calculate the linear and volumetric wear rates based on the previous empirical relations of the bearing surfaces (19–21). Then, these results are compared with the literature data to enhance the reliability of our study. Consequently, this study provides a broader view for the effects of different design parameters on contact mechanics and wear rates of MoM hip implants.

MATERIAL AND METHODS

To understand the effect of parameters on the wear mechanism, a sensitivity analysis is required. The parameters chosen for the sensitivity analysis in this study are as follows: head diameters, cup thicknesses, material combinations, coating materials, and coating thicknesses. Since the wear rate has a direct effect on the overall lifespan of the prosthesis, to quantify these effects, Archard wear equation is utilized to calculate linear and volumetric wear rates based on the previous empirical relations of bearing surfaces (22). The comprehensive investigation of these parameters affecting the contact pressure and its distribution are head radius, cup thickness, material combinations, coating material, and its thickness, respectively. The maximum hip joint contact force in terms of body weight (BW) % during a gait cycle was determined as 368±78 %- BW (23). The hip contact force of a 70-kg person is approximately 2500 N. Therefore, the nominal load of 2500 N is applied at the center of the femoral head, which is approximately 3.5 times the body weight of a 70-kg per person in all prototypes (24). This load is selected as the maximum hip contact force during normal gait cycles (25). Then, the obtained results were compared to the numeric method used by the finite element method.

Analytical Methods

The load *(P)* is calculated by multiplying the contact area relating to the contact radius (a_h) with the contact pressure *(p)* in Eq. 1.

$$P = \pi {a_h}^2 p \tag{1}$$

Equivalent modulus E is replaced by E' as following Eq. 2

$$1/E' = (1-{\upsilon_h}^2)/E + (1-{\upsilon_c}^2)/E_c \tag{2}$$

In this equation υ_h is the head material's Poisson ratio and υ_c is the cup material's Poisson ratio, E_h is the elastic moduli of the head material and E_c is the cup material elastic moduli. The equivalent ball radii (R_{eq}) are related to the head (R_h) and the cup (R_c) surfaces. The equivalent ball radius is determined by Eq. 3:

$$R_{eq} = (R_c\, R_h)/\mathrm{c} \tag{3}$$

where, R_c is a cup radius, R_h is the femoral head radius and c is the radial clearance (Figure 1a). The half contact radius a_h between the head and the cup is calculated by Eq. 4:

$$a_h = (3PR_{eq}\frac{(1-{\upsilon_h}^2)\mathrm{Ec} + (1-{\upsilon_c}^2)\mathrm{Eh}}{E_h E_c})^{\frac{1}{3}} \tag{4}$$

At the same material combination, we can simplify Eq. 5:

$${a_h}^3 = (3PR_{eq}(1-\upsilon^2)/2E) = 0.75(PR_{eq}/E') \tag{5}$$

The maximum contact pressure in Eq. 1 can be simplified in terms of contact radius and load in Eq. 6:

$$p_{max} = (3\mathrm{P}/2\pi {a_h}^2) \tag{6}$$

And the formula based on the horizontal distance (x) for the calculation of the pressure distribution from the contact center is given in Eq. 7:

$$p = p_{max}\,[1-(\frac{x}{a_h})^2]^{1/2} \tag{7}$$

The horizontal distance (x) and the contact radius (a_h) are transformed into the polar coordinate system. In the numerical calculations, x values in the Cartesian coordinate are found using the probe command in ANSYS/Workbench over the acetabular cup surface while the contact half-angle and the angle values are calculated by using the transformation of the horizontal axis (x) and the contact radius into the polar coordinate.

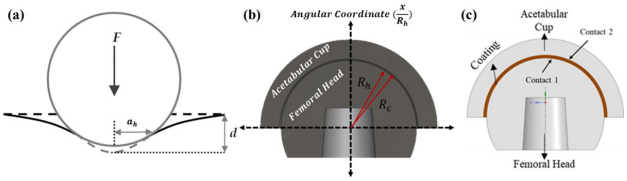

Figure 1 Schematic illustrations of (a) half angle of contact mechanics, (b) uncoated and (c) coated prototypes of the ball-in-socket model.

Numerical Methods

The Finite Element Model (FEM) prototypes are performed as a static model under a constant load of 2500N varying the effect of some parameters such as cup thickness, femoral head radius, material combinations, coating film material combinations and thickness. To understand the effects of contact pressure and pressure distribution on the wear rates in MoM-bearing couples, the sensitivity analysis was performed. Therefore, two different prototypes were modeled and named as coated and uncoated prototypes. The femoral head had a diameter of 36 mm while the clearance between the femoral head and acetabular cup was 50 µm. The acetabular cup thickness was kept constant at 5 mm to minimize the additional effects on contact pressure (8). Additionally, coated prototypes had three different coating thicknesses such as 100, 250, and 500 µm. These prototypes were meshed with Solid186 (26), a quadratic element type with 20 nodes per unit element (27), and each node having 3 different degrees of freedom in ANSYS Inc. 2021

R2 (Canonsburg, PA, USA). The mesh convergence test was performed to determine the number of elements that affect the results of the system analysis the least. For this purpose, the investigated value (contact pressure) was controlled by increasing the number of elements. The prototype with 1-mm mesh size had 42978 elements, 160180 nodes, and 1856 contact elements while the prototype with 2-mm mesh size had 7881 elements, 26890 nodes and 594 contact elements. The detailed mesh convergence tests are shown in Figure 2. The contact pressure was checked by changing the number of contact elements, and the mesh sensitivity analysis was completed when the variation between the previous pressure and the next value was less than 2% (26). Therefore, the optimum mesh size for the two prototypes was selected as 1 mm shown in Figure 2.

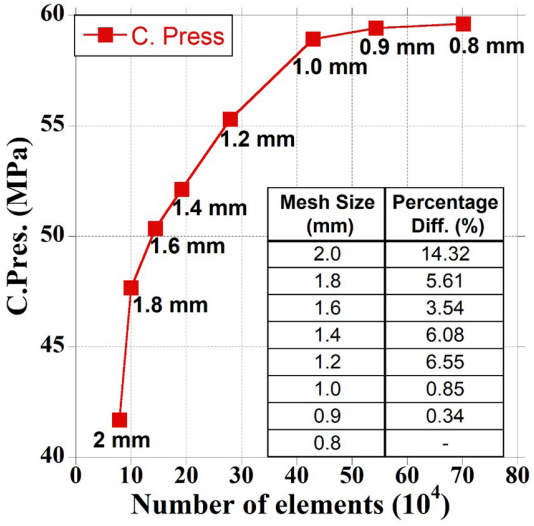

Figure 2 The mesh convergence test result of 36 mm femoral head with 5 mm liner thickness

In uncoated prototypes, Figure 3b, the acetabular cup and femoral head were positioned at $45°$ on the flexion/extension (FE) axis to mimic the neutral position of the acetabular cup with respect to the pelvic bone. In coated prototypes, (Figure 1b) the coating film inserted between the acetabular cup and femoral head was positioned on the flexion/extension (FE) axis to mimic the neutral position of the acetabular cup with respect to the pelvic bone Figure 3b (20,26). The acetabular cup with coating film was rotated $45°$ on the flexion/extension (FE) axis to mimic the neutral position of the acetabular cup with respect to the pelvic bone Figure 3b. In the coated and the uncoated prototypes, acetabular cups were fixed on the outer surface allowing no rotation and translation movement (Figure 3a), while the femoral head was free to move and rotate in each direction (28–30). The load was applied at the bottom side of the femoral head as shown in Figure 3a. The hard-on-hard bearing materials of hip implant materials of the model are available in

Table 1. The prototype simulations were performed under a constant load of 2500N. The acetabular cup and femoral head were positioned at 45° on the flexion/extension (FE) axis to mimic the neutral position of the acetabular cup with respect to the pelvic bone shown in Figure 4.

Table 1 Mechanical properties of hip implant bearing materials.

	Elastic Modulus (GPa)	Poisson Ratio
Stainless Steel (SS) (31)	196	0.30
Ti-6Al-4V (32)	110	0.30
CoCr (26)	220	0.29
Ti12Mo6Zr2Fe (TMZF) (33)	79.5	0.33

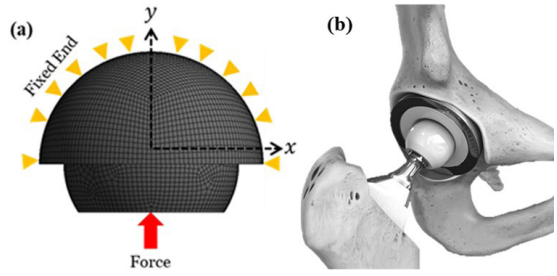

Figure 3 (a) The loading and boundary conditions and (b) total hip replacement of bearing couples

Computational And Analytical Wear

Archard wear equation (22) was used to predict the wear rates of all bearing components in THR. The linear wear depth (W_L) could be described as in Eq. 8

$$W_L = KxPxS \tag{8}$$

It was assumed that linear wear depth (W_L) is accumulated in proportion to the contact pressure (P) and the wear sliding distance (S). K is the dimensionless wear coefficient factor obtained from in vitro studies listed in Table 2 [14]. Similarly, the volumetric wear (W_V) is predicted by multiplying the linear wear depth (W_L) with the contact area (A_{c_i}) (Eq. 9).

$$W_w = W_L \, x \, A_{c_i} \tag{9}$$

In this study, linear and volumetric wear rates of bearing surfaces have been analyzed using analytical and numeric methods. Hip joint contact force (HJCF) and sliding distance (S) of normal gait cycles were obtained from a multibody simulation. The multibody simulations were performed using AnyBody Modeling System, and HJCF was calculated by using inverse dynamic and muscle recruitment optimization algorithms (23). The maximum sliding distance for one gait cycle was determined as a 7.77 mm in the literature (23). Also, it is assumed that an average human gait reaches to one million cycle in a year (11). Therefore, the linear and volumetric wear rates were calculated under this assumption (11,26,27). The coefficients of friction values are listed in Table 2.

In this study, linear and volumetric wear rates of bearing surfaces have been analyzed using analytical and numeric methods. Hip joint contact force (HJCF) and sliding distance

(S) of normal gait cycles were obtained from a multibody simulation. The multibody simulations were performed using AnyBody Modeling System, and HJCF was calculated by using inverse dynamic and muscle recruitment optimization algorithms (23). The maximum sliding distance for one gait cycle was determined as a 7.77 mm in the literature (23). Also, it is assumed that an average human gait reaches to one million cycle in a year (11). Therefore, the linear and volumetric wear rates were calculated under this assumption (11,26,27). The coefficients of friction values are listed in Table 2.

Table 2 The Archard wear factor and coefficient of friction properties of hip implant bearing materials.

	Archard Wear Factor (K) *(mm^3/Nmm)*	CoF
CoCr/CoCr (26)	5×10^{-12}	0.20
CoCr/SS (34)	4.5×10^{-8}	0.15
CoCr/Ti-6Al-4V (35)	1.03×10^{-7}	0.58
CoCr/TMZF (35)	1.03×10^{-8}	0.58

RESULTS AND DISCUSSION

The contact pressure values were estimated as 59.418 *MPa* by the numeric method using FEM and it was calculated as 54.905 *MPa* using Hertz theory as an analytical method as shown in mathematical equations (Figure 4a). The percentage error formulation is used to compare the numerical and analytical results. The percentage error formulation is as follows:

$$Percentage\ error\ (\%) = \frac{Numerical\ result(FEM) - Analytical\ result(Hertz\ Theory)}{Analytical\ result(Hertz\ Theory)} \times 100 \qquad (10)$$

The minimum error using Eq. 10 between the analytical and the numerical calculation was 0.24% for 28 *mm* of the head diameter, while the maximum error was 11.79 % for 48-*mm* of head diameter as shown in Figure 4b. The effects of changing head radius, cup thickness, material combination, and coating thickness are provided in the following part in detail.

Head Radius Effects

The femoral head radius, from 28 to 48-mm, was investigated under 2500 N, whilst the clearance value of 0.05-mm and cup thickness of 5-mm were kept constant to investigate the effect of change of radius on contact pressure and total deformation on the cup bearing surface. The numerical maximum contact pressure value was obtained from the 28-mm head radius at a half contact angle of 150^0 and also its contact area and linear wear were calculated as 53.61 mm^2 and 0.00294mm/Mc respectively, while the analytical maximum result was calculated at a half contact angle of 100^0 and its contact area and linear wear were, 48.89 mm^2 and 0.00298 mm/Mc, respectively. The minimum contact pressure values were obtained from 48-mm of head radius at a half contact angle of 190^0 (contact area of 92.52 mm^2 and volumetric wear of 0.1571 mm^3/Mc and 150 (contact area of 100.25 mm^2 and 0.1454 mm^3/Mc) in FEM and Hertz calculations, respectively. Additionally, the numerical and analytical results are shown in Figure 5 and are listed in Table 3.

Cup Thickness Effects

The effect of cup thickness is investigated in ten prototypes under a constant loading of 2500 N. All prototypes had the same head diameter of 36 mm with a 50 µm clearance. The cup thicknesses varied from 1 to 10 *mm*. The maximum contact pressure was determined as 67.127 *MPa* with 2 *mm* thickness, while the minimum contact pressure was obtained as 56.264 *MPa* with 10 *mm* thickness in the numerical analysis. In analytical results, the contact pressure was affected by changing the cup thickness. So, the percentage error was obtained as 21.6% with a cup thickness of 2-*mm* prototype, while the error in the prototype with a 10- *mm* thickness was only 1.9%. The prototypes with 10 *mm* of cup thickness produced similar contact pressure numerically and analytically. Additionally, pressures calculated analytically

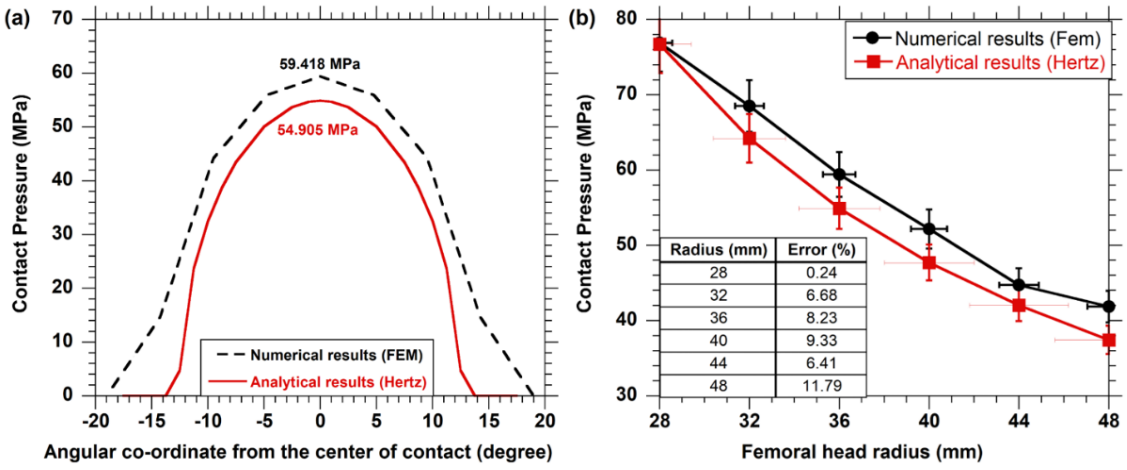

Figure 4 Comparison of numerical and analytical contact pressure of (a) 36 *mm* head radius, and (b) head radius varying from 28 *mm* to 48 *mm*.

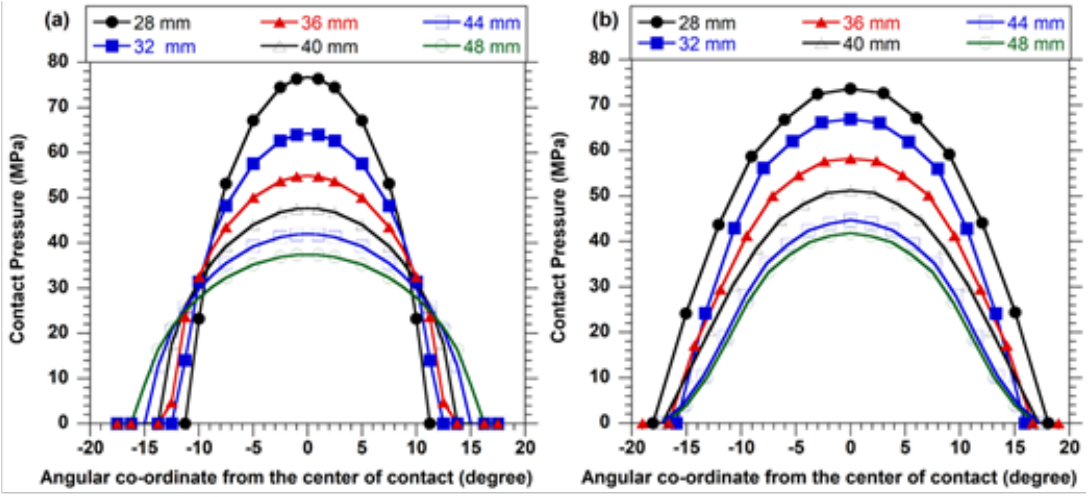

Figure 5 The effect of head radius changes on contact pressure analytical results (Hertz), and (b) numerical results (FEM) (under 2500 N with 0.05 mm clearance and 5 mm cup thickness)

Table 3 Comparison between numerical and analytical results of the femoral head effect,

Head Diameters *(mm)*	Numerical C. Pres. *(mPa)*	Analytical C. Pres. *(mPa)*	Error *(%)*	Numerical Linear wear *(μm/Mc)*	Analytical Linear wear *(μm/Mc)*	Error L.w. *(%)*	Numerical Vol. wear *(mm^3/Mc m)*	Analytical Vol. wear *(mm^3/Mc m)*	Error V.w. *(%)*
28	75.73	76.71	1.27	2.94	2.98	1.27	0.15771	0.14571	8.24
32	68.51	64.22	6.68	2.66	2.49	6.68	0.15097	0.14574	3.59
36	59.42	54.88	8.23	2.31	2.13	8.23	0.15666	0.14576	7.48
40	52.16	47.71	9.33	2.03	1.85	9.33	0.15753	0.14575	8.08
44	44.72	42.03	6.41	1.74	1.63	6.41	0.14720	0.14578	0.97
48	40.45	37.43	8.06	1.57	1.45	8.06	0.14539	0.14578	0.27

were kept constant, while contact pressures calculated by numeric methods were changed with the varying cup thicknesses (Figure 6a). The pressure distribution with respect to the predicted contact half-angle is shown in Figure 6b. The maximum linear wear rate was calculated at 0.0026 mm/Mc at a 1- *mm* cup thickness, while the minimum linear wear rate was 0.0022 mm/Mc at a 10- *mm* cup thickness in numeric methods. The difference between the maximum and minimum linear wear rates was 18.7 %. Also, the maximum and the minimum errors between numerical and analytical methods were 21% and 1.9%, respectively. Similarly, the maximum volumetric wear rate was calculated as 0.17618 mm^3/year at a 1 *mm* cup thickness, while the minimum linear wear rate was 0.0014834 mm^3/Mc at a 10 *mm* cup thickness. The maximum and minimum error of volumetric wear rates between numerical and analytical methods were 20.2% and 1.19%, respectively. The detailed information on the contact pressure and wear rates varying cup thicknesses are listed in Table 4.

The Effects Of Material Combination In Bearing Couples

CoCr material was mostly used in THR applications due to superior mechanical properties and excellent wear performances (36,37). So, all metal-bearing materials mostly used in THR applications were analyzed numerically and analytically in this study. The selected materials were SS, Ti64, and TMZF. Therefore, the effects of material combination with respect to CoCr material were investigated under constant loading of 2500 N. All prototypes had the same head diameter of 36 mm with and 50 μm clearance. The cup thickness was kept constant at 5 *mm* to minimize the effect of cup thickness. These analyzes are examined in two groups by changing the head and cup materials.

The maximum contact pressure was calculated as 57.65 *MPa* using the numerical and 52.87 *MPa* using the analytical methods for CoCr-on-SS, while contact pressures were 43.10 *MPa* in the numerical and 36.46 *MPa* in the analytical methods for CoCr-on-TMZF bearing couple. The maximum linear wear rates were obtained as 45.602 mm/year in the numerical and 33.613 mm/Mc in the analytical methods for CoCr-on-Ti64, the minimum linear wear rates were 20.157 mm/year in the numerical and 18.486 mm/Mc in the analytical methods for CoCr-on-SS. The maximum and minimum errors of linear wear rates between the numerical and analytical methods were 35.67 % and 9.04%, respectively. Similarly, the maximum volumetric wear rates were 3094.76 mm^3/Mc in the numerical and 2297.07 mm^3/Mc in the analytical methods for CoCr-on-Ti64, the minimum volumetric wear rates were as 1367.98

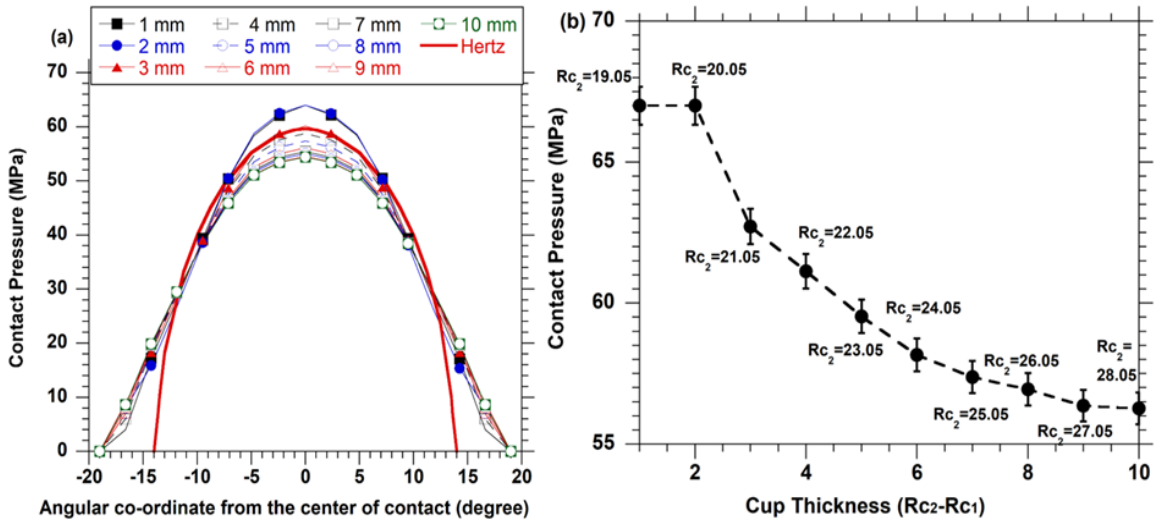

Figure 6 Contact pressure vs (a) half contact angle, and (b) cup thickness.

mm³/Mc in the numerical and 1263.31 mm³/Mc in the analytical methods for CoCr-on-SS. The maximum and minimum errors of volumetric wear rates between the numerical and the analytical methods were 34.73 % and 8.29%, respectively. The detailed information on the contact pressure and wear rates of varying material combinations are listed in Table 5.

Coating Film Material Combinations And Thickness

The effects of the coating material and optimum coating thickness were examined using the prototypes which had a femoral head diameter of 36 *mm*, clearance of 0.05 *mm*, under the loading of 2500 N. Using three different coating materials, SS, Ti6Al4V, and TMZF, respectively CoCr acetabular cup surfaces were coated by varying coating thicknesses of 100 µm, 250 µm, and 500 µm. In total, 9 prototypes were designed. After running the simulations with nine prototypes using finite element method (FEM), the contact areas were 68.33 mm² for CoCr/CoCr, 70.94 mm² for CoCr/SS, 89.29 mm² for CoCr/Ti64 and 102.84 mm² for CoCr/TMZF for all coating thicknesses, respectively. The highest contact pressure on cup surfaces with SS coating material was 53.6 *MPa* with a coating thickness of 100 µm as listed in Table 6, while the minimum contact pressure on cup surfaces with TMZF coating material was 39.6 MPa with a coating thickness of 500 µm. The maximum number of cycles required to remove for each coating material on cup surfaces are given in Table 6. The maximum survival cycles of coating material is obtained approximately as 32000 cycles at the SS coated cup with 500 µm coating thickness. However, the minimum survival cycles of coating material is obtained as 2532 cycles at the TMZF

Table 4 The effect of cup thicknesses on contact pressures

Cup Thick (*mm*)	Num. C.Pres. (*MPa*)	Ana. C. Pres. (*MPa*)	Error (%)	Numerical Linear wear (*µm/Mc*)	Analytical Linear wear (*mm/Mc*)	Error L.w. (%)	Numerical Vol. wear (*mm³/Mc*)	Analytical Vol. wear (*mm³/Mc*)	Error V.w. (%)
1	66.823		21.023	2.60		21.023	0.17618		20.18
2	67.127		21.574	2.61		21.574	0.17698		20.73
3	62.714		13.581	2.44		13.581	0.16535		12.79
4	61.124		10.702	2.37		10.702	0.16116		9.93
5	59.521		7.799	2.31		7.799	0.15693		7.05
6	58.159	54.88	5.332	2.26	2.15	5.332	0.15334	0.14659	4.60
7	57.375		3.912	2.23		3.912	0.15127		3.19
8	56.939		3.122	2.21		3.122	0.15012		2.41
9	56.355		2.065	2.19		2.065	0.14858		1.36
10	56.264		1.900	2.19		1.900	0.14834		1.19

Table 5 The effects of the material combinations on contact pressures (analytical (Hertz), and (b) numerical results (FEM))

Bearing Couple		Num. C. P.	Ana. C. P.	Num. L.w	Ana. L.w	Error L.w.	Num. V.w.	Ana. V.w.	Error V.w.
Head	Cup	*(MPa)*	*(MPa)*	$\left(\frac{\mu m}{Mc}\right)$ X1000	$\left(\frac{\mu m}{Mc}\right)$ X1000	(%)	(mm^3/Mc)	(mm^3/Mc)	(%)
CoCr	SS	57.65	52.87	20.157	18.486	9.041	1367.98	1263.31	8.29
CoCr	Ti64	47.92	42.00	38.351	33.613	14.095	2602.68	2297.07	13.30
CoCr	TMZF	43.10	36.46	34.493	29.179	18.212	2340.89	1994.08	17.39
SS	CoCr	59.42	52.87	20.776	18.486	12.389	1409.98	1263.31	11.61
Ti64	CoCr	56.98	42.00	45.602	33.613	35.667	3094.76	2297.07	34.73
TMZF	CoCr	44.37	36.46	35.510	29.179	21.695	2409.87	1994.08	20.85

coated cup with 100 µm coating thickness.
The main purpose of this study is to analyze the parameters affecting the contact pressure on metal-on-metal (MoM)

Table 6 Contact pressure and linear and volumetric wear rates of three coating materials varying with different coating thickness.

Coating Thickness	SS	Ti64	TMZF	SS	Ti64	TMZF
	Contact Pressure			Max cycles to remove coating material		
(µm)	*(MPa)*			*(cycles)*		
100	53.6	53.0	49.3	5348	2359	2532
250	48.2	47.1	39.6	14793	6631	7886
500	44.8	43.5	39.5	31847	14368	15823

implants using analytical and numerical methods as a part of the verification process for the contact pressure values. Moreover, to compare the effects of the parameters on contact pressure, the contact radius and the contact area values were calculated using Hertz contact theory analytically, while these results were also obtained using the numerical output of finite element method (FEM) numerically Additionally, the effects of different design parameters such as head diameters, bearing material combinations, coating materials and their thickness on contact pressure were analyzed. And these results were used in the calculation of linear and volumetric wear rates of MoM bearing couples.

The contact pressure of ceramic-on-ceramic bearing components (9) had an error of 30% between the analytical and numerical solutions, while the metal-on-polyethylene bearing couple model (38) had an error of 27.5%. In our study, the percentage error was calculated as 4.9% under the same loading and boundary conditions and also the same geometrical dimensions in the literature (9,38). A similar situation was encountered in calculations of half contact angle; for example, while the error is about 26.7% in the clearance calculations, this is about 25% in head radius calculations. Although Hertz contact theory is frequently used in the design of hip implants for understanding contact mechanics [10]–[12],[19]–[23], the effects of cup or coating thickness on the contact pressure and predicting wear estimation have not been studied. Hertz contact theory is only based on the inferences of contacting surfaces (22,40).

Similarly, there are many studies on the effect of head size using numerical and experimental methods in the literature (38,41–44). These studies conclude that the contact pressure increases with the decreasing head size and the volumetric wear increases with the decrease of the head size based on the Hertz contact theory. Keeping the head size constant with a thicker liner and the coating material corresponds to a lower peak contact stress and larger contact area. Increases in the contact area result in higher wear rates of bearing couples (41–44).

Our results are also in line with these results as demonstrated in the results section. When the MoM bearing components have a larger diameter, the volumetric wear rates of bearing surfaces are reduced (43,44). For the 36 mm head size model under 2500 N, the contact pressure and the contact area are 54.52 MPa and 76.25 mm^2 respectively, in the numeric model and 54.9 MPa and 77.16 mm^2 in the analytic model, respectively. In the literature, for 39 mm femoral head size, the contact pressure was calculated as 40 MPa with a contacting area of 74 mm^2(44). When the head size increases, the errors between the numeric and the analytic results increase. One of the most important reasons for these errors is that the prototypes with higher head sizes have a higher number of contact elements and higher moments of inertia. Therefore, the contact elements under the same loading conditions results in more fluctuations and penetration at the contact surfaces. However, these situations are not valid in analytical studies. Because Hertz contact theory, as analytical study, only considers the contact surfaces as a 2-dimensional geometry, while the numerical studies are performed in 3-dimensional geometry including the inertia, mass, moment, variables etc. (22,41).

In our study, the effects of cup thickness ranging from 1 to 10 mm were analyzed numerically and analytically. The pressure on the cup bearing surface decreased exponentially by increasing the cup thickness and continued up to 9 mm of the cup thickness. At 10 mm of the cup thickness parameter value, the cup thicknesses parameter had no effect on the output, and the difference between the numerical results and the analytical results decreased from 21.02 to 1.9 percent. In Hertz contact theory, the contact pressure is kept constant while changing the cup thickness, since this theory only focuses on the effect of contacting the bearing surface. However, this

assumption cannot be valid for the numerical results, since in the numeric approach the mass and volume parameters are included using FEM.

The linear wear rates of CoCr-on-CoCr bearing couples were obtained at 2.5 µm/Mc (26). In another study in the literature, the predicted total linear wear was calculated as 1.28 µm/Mc and the maximum Hertzian contact radius as 3.94 mm, while the CoCr head diameter is 27.899 mm with a 79 µm clearance under applied loading of 2085 N (45). Another study shows that the linear wear rates ranged from 2.9 to 12.8 µm/Mc, with the femoral head radius of 14 mm (46). These results are consistent with our study. In our study, the linear wear was obtained as 2.98 µm/Mc in analytical methods and 2.98 µm/Mc in numerical methods, while the maximum contact radius was calculated as 3.945 mm in analytical methods and estimated as 4.13 mm in numeric methods.

The materials mostly used in THR application against CoCr material are also analyzed in numerical and analytical methods. These materials are SS, Ti6Al4V, and TMZF, respectively. The maximum contact pressure was 59.42 MPa for CoCr-CoCr bearing couple, while the minimum contact pressure value was 43.10 MPa for CoCr-TMZF bearing couple. It produced the same results about contact pressures and contact areas analytically whether the bearing pairs were made of CoCr (head)-SS (cup) or SS (head)-CoCr(cup). However, it produced different pressure and contact areas in numeric methods when the bearing couples changed. When the head material of CoCr and cup material of SS is selected, the contact pressure, the linear wear, and the volumetric wear rates were 57.65 MPa, 20157 µm/Mc, 1367.98 mm^3/Mc, respectively. The errors of linear and volumetric wear rates between the numeric and the analytic methods were 9.041% and 8.29%, respectively. When the head material of SS and cup material of CoCr was selected, the contact pressure, linear wear, and volumetric wear rates were 59.42 MPa, 20776 µm/Mc, 1409.98 mm^3/Mc, respectively. The errors of linear and volumetric wear rates between numeric and analytic methods were increased from 9.04 to 12.4% and from 8.29 to 11.61%, respectively. These differences were observed to have depended on the material combination of the bearing couple. Unfortunately, these results could not be compared to the data in the literature. Because there has not been any other study providing a comparison of changing bearing couples.

The effects of coating material and coating thickness on contact pressure, and linear and volumetric wear rates were also analyzed in our study. Three different coating thicknesses were modelled with three different coating materials. The coating thickness was chosen as 100µm, 250µm ve 500 µm, and the coating materials are SS, Ti6Al4V, and TMZF respectively. The maximum contact pressure was obtained as 53.6 MPa when coated with 100 µm coating thickness of SS, while the minimum contact pressure was obtained as 39.6 MPa with 500 µm coating thickness of TMZF. The coating thickness directly affected the contact pressure, the linear wear, and the volumetric wear rates. Also, the coating thickness of 500 µm for all the bearing couples had the lowest contact pressure and the linear and volumetric wear rates. It was observed that the metallic coating materials used in this study were insufficient considering higher wear rates for hip implants application. Our results are compared and considered to be consistent with the literature (47,48).

The analytical data is consistent with numerical data under the same loading and boundary conditions. To understand the effect of contact pressure on linear and volumetric wear depth, we calculated the wear rates over one million cycles. This study focuses on the primary results of contact pressure and then uses this information to compare the primary effects of contact pressure on wear rates. In our study, analytic and numeric models assumed smooth bearing surface and constant friction coefficients. Since Hertz contact theory is only valid on a non-adhesive and elastic contact on smooth surfaces (13,40). However, the bearing surfaces can form a rough surface and worn geometry depending on the wear depth (26,27). Also, the coefficient of friction in reality, is known to be changing and not constant (37). These problems will be addressed in future studies. Despite these limitations, this study provides useful information for implant designers while optimizing their products as they lead to low contact pressures. This study could open a new window into understanding the initial effects of geometrical parameters and material combination on lifespan of different THR implants while analyzing any other futuristic properties.

CONCLUSION

In this study, we demonstrated contact mechanics and wear rates of bearing couples using numeric and analytic methods. The effect of head size, cup thickness, material combination of bearing couple, coating material, and film thickness on contact pressure distribution and wear rates were investigated in detail. The cup thickness was observed to have a significant effect on the contact pressure, linear and volumetric wear rates of bearing couples. When the cup thickness was selected as 10 mm, the contact pressure and wear rates decreased by 16% approximately. Additionally, the error between the numeric and analytic results decreased from 21.02 to 1.9% for the contact pressure and from 20.18 to 1.19% for the volumetric wear rates. Similarly, optimum selection of the material combination of bearing couples decreased the contact pressure by 27%. Although the material combination had no positive effect on the wear rates of bearing surfaces, it could be minimizing the stress shielding effects of the bone underneath the hip implants. It is concluded when the film thickness increases from 100 to 500 µm, 18-20% decrease in the contact pressure and linear and volumetric wear rates were observed for all the coating materials, The methodology and the results used in this study, could be useful for implant designers during design optimization studies.

Acknowledgement

The study was supported by the TUBITAK 2232 Funding program under the name of '118C188 New Generation Implants for All' project.

References

1. Merola M, Affatato S. Materials for hip prostheses: A review of wear and loading considerations. Materials. 2019;12(3).
2. Charnley J, Cupic Z. The Nine and Ten Year Results of the Low-

Friction Arthroplasty of the Hip. Clinical Orthopaedics and Related Research®. 1973;95.
3. McKee GK, Watson-Farrar J. REPLACEMENT OF ARTHRITIC HIPS BY THE McKEE-FARRAR PROSTHESIS. The Journal of Bone and Joint Surgery British volume [Internet]. 1966 May 1;48-B(2):245–59. Available from: https://doi.org/10.1302/0301-620X.48B2.245
4. Smith SL, Dowson D, Goldsmith AAJ. The lubrication of metal-on-metal total hip joints: A slide down the Stribeck curve. Proceedings of the Institution of Mechanical Engineers, Part J: Journal of Engineering Tribology [Internet]. 2001 May 1;215(5):483–93. Available from: https://doi.org/10.1243/1350650011543718
5. Learmonth ID, Gheduzzi S, Vail TP. Clinical experience with metal-on-metal total joint replacements: Indications and results. Proceedings of the Institution of Mechanical Engineers, Part H: Journal of Engineering in Medicine [Internet]. 2006 Feb 1;220(2):229–37. Available from: https://doi.org/10.1243/095441105X69123
6. Fisher J, Bell J, Barbour PSM, Tipper JL, Mattews JB, Besong AA, et al. A novel method for the prediction of functional biological activity of polyethylene wear debris. Proceedings of the Institution of Mechanical Engineers, Part H: Journal of Engineering in Medicine [Internet]. 2001 Feb 1;215(2):127–32. Available from: https://doi.org/10.1243/0954411011533599
7. National Joint Registry for England Wales Northern Ireland and the Isle of Man. 16th Annual Report 2019:National Joint Registry for England, Wales, Northern Ireland and the Isle of Man. NJR 16th Annual Report 2019 [Internet]. 2019;(December 2018):1–248. Available from: https://www.hqip.org.uk/wp-content/uploads/2018/11/NJR-15th-Annual-Report-2018.pdf
8. Mak MM, Jin ZM. Analysis of contact mechanics in ceramic-on-ceramic hip joint replacements. Proceedings of the Institution of Mechanical Engineers, Part H: Journal of Engineering in Medicine [Internet]. 2002 Apr 1;216(4):231–6. Available from: https://doi.org/10.1243/09544110260138718
9. Cilingir AC. Finite element analysis of the contact mechanics of ceramic-on-ceramic hip resurfacing prostheses. Journal of Bionic Engineering [Internet]. 2010;7(3):244–53. Available from: http://dx.doi.org/10.1016/S1672-6529(10)60247-8
10. Chethan KN, Shyamasunder Bhat N, Zuber M, Satish Shenoy B. Finite element analysis of hip implant with varying in taper neck lengths under static loading conditions. Computer Methods and Programs in Biomedicine [Internet]. 2021;208:106273. Available from: https://doi.org/10.1016/j.cmpb.2021.106273
11. K N C, Ogulcan G, Bhat N S, Zuber M, Shenoy B S. Wear estimation of trapezoidal and circular shaped hip implants along with varying taper trunnion radiuses using finite element method. Computer Methods and Programs in Biomedicine [Internet]. 2020;196:105597. Available from: https://doi.org/10.1016/j.cmpb.2020.105597
12. Pandiyarajan R, Starvin MS, Ganesh KC. Contact Stress Distribution of Large Diameter Ball Bearing Using Hertzian Elliptical Contact Theory. Procedia Engineering [Internet]. 2012;38:264–9. Available from: https://www.sciencedirect.com/science/article/pii/S1877705812019479
13. Wang QJ, Zhu D. Hertz Theory: Contact of Spherical Surfaces BT - Encyclopedia of Tribology. In: Wang QJ, Chung Y-W, editors. Boston, MA: Springer US; 2013. p. 1654–62. Available from: https://doi.org/10.1007/978-0-387-92897-5_492
14. Mihçin Ş, Ciklacandir S. TOWARDS INTEGRATION OF THE FINITE ELEMENT MODELING TECHNIQUE INTO BIOMEDICAL ENGINEERING EDUCATION. Biomedical Engineering: Applications, Basis and Communications [Internet]. 2021 Nov 3;2150054. Available from: https://doi.org/10.4015/S101623722150054X
15. Göktaş H, Subaşi E, Uzkut M, Kara M, Biçici H, Shirazi H, et al. Optimization of Hip Implant Designs Based on Its Mechanical Behaviour BT - Biomechanics in Medicine, Sport and Biology. In: Hadamus A, Piszczatowski S, Syczewska M, Błażkiewicz M, editors. Cham: Springer International Publishing; 2022. p. 37–43.
16. Celik E, Alemdar F, Bati M, Dasdemir MF, Buyukbayraktar OA, Chethan KN, et al. Mechanical Investigation for the Use of Polylactic Acid in Total Hip Arthroplasty Using FEM Analysis BT - Biomechanics in Medicine, Sport and Biology. In: Hadamus A, Piszczatowski S, Syczewska M, Błażkiewicz M, editors. Cham: Springer International Publishing; 2022. p. 17–23.
17. Mihcin S, Sahin AM, Yilmaz M, Alpkaya AT, Tuna M, Akdeniz S, et al. Database covering the prayer movements which were not available previously. Scientific Data [Internet]. 2023;10(1):276. Available from: https://doi.org/10.1038/s41597-023-02196-x
18. Hertz H. Ueber die Berührung fester elastischer Körper. Ueber die Berührung fester elastischer Körper [Internet]. 1882; Available from: https://www.degruyter.com/document/doi/10.1515/crll.1882.92.156/html
19. Alpkaya AT, Mihcin S. Dynamic computational wear model of PEEK-on-XLPE bearing couple in total hip replacements. Medical Engineering & Physics [Internet]. 2023;104006. Available from: https://www.sciencedirect.com/science/article/pii/S1350453323000619
20. Alpkaya AT, Mihçin Ş. The Computational Approach to Predicting Wear: Comparison of Wear Performance of CFR-PEEK and XLPE Liners in Total Hip Replacement. Tribology Transactions [Internet]. 2023;66(1):59–72. Available from: https://doi.org/10.1080/10402004.2022.2140727
21. Alpkaya AT, Yılmaz M, Şahin AM, Mihçin DŞ. Investigation of stair ascending and descending activities on the lifespan of hip implants. Medical Engineering and Physics. 2024;126.
22. Archard JF, Hirst W, Allibone TE. The wear of metals under unlubricated conditions. Proceedings of the Royal Society of London Series A Mathematical and Physical Sciences [Internet]. 1956 Aug 2;236(1206):397–410. Available from: https://doi.org/10.1098/rspa.1956.0144
23. Varady PA, Glitsch U, Augat P. Loads in the hip joint during physically demanding occupational tasks: A motion analysis study. Journal of Biomechanics [Internet]. 2015;48(12):3227–33. Available from: http://dx.doi.org/10.1016/j.jbiomech.2015.06.034
24. Bergmann G, Graichen F, Rohlmann A. Hip joint loading during walking and running, measured in two patients. Journal of Biomechanics. 1993;26(8):969–90.
25. Bergmann G, Bergmann G, Deuretzabacher G, Deuretzabacher G, Heller M, Heller M, et al. Hip forces and gait patterns from rountine activities. Journal of Biomechanics. 2001;34:859–71.
26. Uddin MS, Zhang LC. Predicting the wear of hard-on-hard hip joint prostheses. Wear [Internet]. 2013;301(1–2):192–200. Available from: http://dx.doi.org/10.1016/j.wear.2013.01.009
27. Nithyaprakash R, Shankar S, Uddin MS. Computational wear assessment of hard on hard hip implants subject to physically demanding tasks. Medical and Biological Engineering and Computing. 2018;56(5):899–910.
28. Strickland MA, Dressler MR, Taylor M. Predicting implant UHMWPE wear in-silico: A robust, adaptable computational-

numerical framework for future theoretical models. Wear [Internet]. 2012;274–275:100–8. Available from: http://dx.doi.org/10.1016/j.wear.2011.08.020
29. Ming Song ST, Ashkanfar A, English R, Rothwell G. Computational method for bearing surface wear prediction in total hip replacements. Journal of the Mechanical Behavior of Biomedical Materials. 2021 Jul 1;119.
30. Ruggiero A, Sicilia A. Lubrication modeling and wear calculation in artificial hip joint during the gait. Tribology International [Internet]. 2020;142(September 2019):105993. Available from: https://doi.org/10.1016/j.triboint.2019.105993
31. Bhatt H, Goswami T. Implant wear mechanisms - Basic approach. Biomedical Materials. 2008;3(4).
32. Güden M, Alpkaya AT, Hamat BA, Hızlı B, Taşdemirci A, Tanrıkulu AA, et al. The quasi-static crush response of electron-beam-melt Ti6Al4V body-centred-cubic lattices: The effect of the number of cells, strut diameter and face sheet. Strain. 2022;58(3):1–20.
33. Yang X, Hutchinson CR. Corrosion-wear of β-Ti alloy TMZF (Ti-12Mo-6Zr-2Fe) in simulated body fluid. Acta Biomaterialia [Internet]. 2016;42:429–39. Available from: http://dx.doi.org/10.1016/j.actbio.2016.07.008
34. Chen Y, Wu JM, Nie X, Yu S. Study on failure mechanisms of DLC coated Ti6Al4V and CoCr under cyclic high combined contact stress. Journal of Alloys and Compounds [Internet]. 2016;688:964–73. Available from: http://dx.doi.org/10.1016/j.jallcom.2016.07.254
35. Zhang T, Harrison NM, McDonnell PF, McHugh PE, Leen SB. A finite element methodology for wear-fatigue analysis for modular hip implants. Tribology International [Internet]. 2013;65:113–27. Available from: http://dx.doi.org/10.1016/j.triboint.2013.02.016
36. Heuberger R, Stöck C, Sahin J, Eschbach L. PEEK as a replacement for CoCrMo in knee prostheses: Pin-on-disc wear test of PEEK-on-polyethylene articulations. Biotribology. 2021 Sep 1;27.
37. Scholes SC, Unsworth A. Wear studies on the likely performance of CFR-PEEK/CoCrMo for use as artificial joint bearing materials. Journal of Materials Science: Materials in Medicine. 2009 Jan;20(1):163–70.
38. Askari E, Andersen MS. A closed-form formulation for the conformal articulation of metal-on-polyethylene hip prostheses: Contact mechanics and sliding distance. Proceedings of the Institution of Mechanical Engineers, Part H: Journal of Engineering in Medicine [Internet]. 2018 Nov 16;232(12):1196–208. Available from: https://doi.org/10.1177/0954411918810044
39. Meng Q, Liu F, Fisher J, Jin Z. Contact mechanics and lubrication analyses of ceramic-on-metal total hip replacements. Tribology International [Internet]. 2013;63:51–60. Available from: http://dx.doi.org/10.1016/j.triboint.2012.02.012
40. Baxter JW, Bumby JR, Johnson KL. One Hundred Years of Hertz Contact. Proceedings of the Institution of Mechanical Engineers [Internet]. 1982 Jun 1;196(1):363–78. Available from: https://doi.org/10.1243/PIME_PROC_1982_196_039_02
41. Li G, Peng Y, Zhou C, Jin Z, Bedair H. The effect of structural parameters of total hip arthroplasty on polyethylene liner wear behavior: A theoretical model analysis. Journal of Orthopaedic Research. 2020;38(7):1587–95.
42. Tarasevicius S, Robertsson O, Kesteris U, Kalesinskas RJ, Wingstrand H. Effect of femoral head size on polyethylene wear and synovitis after total hip arthroplasty: A sonographic and radiographic study of 39 patients. Acta Orthopaedica. 2008;79(4):489–93.
43. Masaoka T, Clarke IC, Yamamoto K, Tamura J, Williams PA, Good VD, et al. Validation of volumetric and linear wear-measurement in UHMWPE cups - A hip simulator analysis. Wear. 2003;254(5–6):391–8.
44. Fisher J. Bioengineering reasons for the failure of metal-on-metal hip prostheses. The Journal of Bone and Joint Surgery British volume. 2011;93-B(8):1001–4.
45. Medley JB, Chan FW, Krygier JJ, Bobyn D. Comparison of alloys and designs in a hip simulator study of metal on metal implants. Clinical Orthopaedics and Related Research. 1996;329(SUPPL.):148–59.
46. Reinisch G, Judmann KP, Lhotka C, Lintner F, Zweymüller KA. Retrieval study of uncemented metal-metal hip prostheses revised for early loosening. Biomaterials. 2003;24(6):1081–91.
47. Guu YY, Lin JF, Ai CF. The tribological characteristics of titanium nitride coatings part i. Coating thickness effects. Wear. 1996;194(1–2):12–21.
48. Lin J, Sproul WD, Moore JJ, Lee S, Myers S. High rate deposition of thick CrN and Cr2N coatings using modulated pulse power (MPP) magnetron sputtering. Surface and Coatings Technology [Internet]. 2011;205(10):3226–34. Available from: http://dx.doi.org/10.1016/j.surfcoat.2010.11.039